Transparent Conductors from Layer-by-Layer Assembled SWNT Films: Importance of Mechanical Properties and a New Figure of Merit

Bong Sup Shim,[†,⊥] Jian Zhu,[†] Edward Jan,[†] Kevin Critchley,[†] and Nicholas A. Kotov[†,‡,§,*]

[†]Department of Chemical Engineering, [‡]Department of Materials Science, and [§]Department of Biomedical Engineering, University of Michigan, Ann Arbor, Michigan, 48109. [⊥]Current address: Materials Science and Engineering, University of Delaware, Newark, Delaware 19716.

ABSTRACT New transparent conductors (TCs) capable of replacing traditional indium tin oxide (ITO) are much needed for displays, sensors, solar cells, smart energy-saving windows, and flexible electronics. Technical requirements of TCs include not only high electrical conductivity and transparency but also environmental stability and mechanical property which are often overlooked in the research environment. Single-walled carbon nanotube (SWNT) coatings have been suggested as alternative TC materials but typically lack sufficient wear resistance compared to ITO. Balancing conductance, transparency, durability, and flexibility is a formidable challenge, which leads us to the introduction of a new TC figure of merit, Π_{TC}, incorporating all these qualities. Maximization of Π_{TC} to that of ITO or better can be suggested as an initial research goal. Fine tuning of SWNT layer-by-layer (LBL) polymeric nanocomposite structures makes possible integration of all the necessary properties. The produced TC demonstrated resistivity of 86 Ω/sq with 80.2% optical transmittance combined with tensile modulus, strength, and toughness of the film of 12.3 ± 3.4 GPa, 218 ± 13 MPa, and 8 ± 1.7 J/g, respectively. A new transparent capping layer to conserve these properties in the hostile environment with matching or better strength, toughness, and transparency parameters was also demonstrated. Due to application demands, bending performance of TC made by LBL was of special interest and exceeded that of ITO by at least 100 times. Cumulative figure of merit Π_{TC} for the produced coatings was 0.15 Ω^{-1}, whereas the conventional ITO showed $\Pi_{TC} < 0.07$ Ω^{-1}. With overall electrical and optical performance comparable to ITO and exceptional mechanical properties, the described coatings can provide an excellent alternative to ITO or other nanowire- and nanotube-based TC specifically in flexible electronics, displays, and sensors.

KEYWORDS: transparent conductors · transparent conductive coating · nanocomposites · flexible conductors · conductive thin films · carbon nanotubes · layer-by-layer assembly

Transparent conductors (TCs) are one of the most widely used essential electronic materials since 1907 with the first introduction of cadmium oxides.[1] Currently, metal oxides, such as indium tin oxide (ITO), are the TC material of choice with excellent TC performance, which can be evaluated by traditional TC figure of merit, TCFM = σ/α, where σ is electrical conductivity and α is the visible absorption coefficient.[2] The rapid growth of TC applications, however, requires not only high transparency and electrical conductivity but also mechanical flexibility, toughness, property tunability, environmental stability under different conditions, and low processing cost. New generation electronics[3] exemplified by bendable displays, solar cells, and large-area pressure detectors as well as some more exotic applications,[4] including hemispherical cameras, tunable contact lenses, camouflage skins, wearable touch screens, and many others will further require a complex combination of physical properties, among which the central ones are electrical, mechanical, and gas permeation properties. Low temperature and nonvacuum processing also becomes significant lately from the perspective of energy expenditures. Rigid films of conventional glass-like metallic oxides have difficulties satisfying these requirements. Additionally, the cost of indium soared recently due to its relative rareness combined with great increase in demand.[5] Thus, further development of a number of technologies critical for finding a solution for energy problems, such as flexible solar cells, is impeded due to unfavorable cost projections strongly affected by the cost of ITO. The search for ITO replacements with potentially improved mechanical properties to accommodate highly flexible substrates becomes urgent with high priority.

Single-walled carbon nanotube (SWNT) coatings have been introduced to fill the technological gaps of oxide-based conventional TCs.[6,7] Superior physicochemical properties of individual SWNTs, and particularly high electrical conductivity estimated at 10^4-10^6 S/cm,[8−10] make them promising candidates for TCs. For comparison, the electrical conductivity of the state-of-the-art ITO is around 9×10^3 S/cm.[11]

*Address correspondence to kotov@umich.edu.

Received for review January 6, 2010 and accepted May 27, 2010.

Published online June 16, 2010. 10.1021/nn100026n

The challenge of using carbon nanotubes in TC applications, however, is their strong light absorption, and thus, transparency must be achieved by nanoscale thickness of the coating. Nanotube-based TCs can be described as 2D networks of SWNTs which provide both electrical charge carriers and percolating conduction routes.[12,13] Due to thinness of SWNT films necessary for TCs, the processing methods with nanoscale structure control of the coating are exceptionally important. They determine, to a large extent, the degree of nanotube exfoliation and "connectedness",[14] which, in turn, sets the heights of tunneling barriers for charge carrier transfer between the individual tubes.[15] All of these structural parameters affect both σ and α. Efforts have been directed on forming SWNT-only structures mostly by solution processing techniques such as spraying,[16,17] spin-coating,[18] electrophoretic deposition,[19] and filtration.[6,20] Direct synthesis of SWNTs for transparent electronics[21,22] and dry spinning transparent sheet from multiwalled carbon nanotube (MWNT) forests[23] were also demonstrated as nonsolvent techniques.

Strong light absorption of nanotubes imposes significant restrictions on the thickness of coatings and simultaneously increases the requirements for their mechanical properties. The individual SWNTs do possess superb mechanical properties; $E \sim 1$ TPa and $\sigma_{ult} \sim 63$ GPa.[24] They can also undergo very high plastic deformation under stress.[25] However, translation of these properties observed for an individual nanotube should not be automatically assumed for macroscopic SWNT TCs. In fact, most of SWNT TCs described above are not durable enough and their conductivity quickly deteriorates even under mild wear conditions. As such, the strength of bucky papers, the most common SWNT-only sheets by filtration, whose structure is very similar to many TC coatings made from nanotubes, is quite low (*i.e.* $\sigma_{ult} \sim 10-74$ MPa). Also important is that these SWNT mats are brittle rather than flexible, displaying values of strain to failure not exceeding 0.5−5%.[26,27] Overall, one can see that the mechanical properties of ITO alternatives from SWNTs are insufficiently characterized. Finding a method of SWNT TCs that could display high values of TCFM, strength, resistance to wear, and flexibility simultaneously is critical for practical realization of roll-to-roll solar cells and flexible electronics for which SWNT TCs are projected.

The art of combining mechanical, optical, and electrical properties lies in the accurate control of the nanoscale structure of a coating. For instance, the improvement of diverse mechanical characteristics of TCs requires inclusion of adhesive polymer in the structure of a film. However, a mechanically advantageous adhesive always jeopardizes high σ values and versatile properties of SWNT networks. Thus, any compositional reinforcement only accentuates the importance of fine structural tuning. Previously, we presented layer-by-layer assembly (LBL) of SWNTs as a method for TC applications with integrated strength and conductivities.[15] LBL is one of a few thin-film deposition techniques that allow one to control the structure of the coatings with actual nanometer scale precision, which includes both normal[28] and lateral[29] packing of the nanoscale building blocks in the coatings. Consequently, LBL presents exceptional possibilities to satisfy seemingly impossible to combine multiple requirements including transparency, charge transport, environmental resilience, bending strain, and wear resistance.

In this communication, we seek to accomplish two goals: (1) to draw attention to the importance of cumulative evaluation of the performance of any promising TC coating, and (2) to demonstrate the possibility of reaching an extended set of specifications for TC aimed at flexible electronics and superior to ITO and other materials. Along these lines, we propose replacing the traditional figure of merit for TC evaluation with a new one which incorporates measure of mechanical performances. It is important to note that mathematical expressions combining different parameters in the figure of merit may vary, but the idea of obtaining a cumulative numerical value including mechanical properties is essential.

To demonstrate technical feasibility of a new generation TC designed for flexible electronic devices, we report advanced SWNT LBL coatings and apply the new figure of merit for their comparison. In terms of traditional electrical and optical performance parameters, they display 80.2 ± 0.1% in light transmittance (T at λ = 550 nm) and 86 ± 1 ΩU/sq (or Ω/□) in surface resistivity (R_s), which match or even exceed those obtained for analogous SWNT TCs reported so far.[16,22,30−32] Tensile modulus, strength, and toughness of the film were evaluated to be 12.3 ± 3.4 GPa, 218 ± 13 MPa, and 8 ± 1.7 J/g, respectively, which is likely to exceed most current SWNT- and NW-based TC alternatives. Due to importance of flexibility, we were particularly interested in their bending performance. Compared to ITO and bucky-paper-type TCs, it was particularly remarkable to observe the improvement of the maximum bending strain before electrical failure by 100 times. Additionally, the manufacturing technique used here makes it possible to add a long lasting protective capping layer against dedoping and damaging by environmental factors with matching or better mechanical properties. The capping layer is formed without sacrificing their original optical transparency and conductivity. Although, refinement of the structure is still needed to exceed the performance of ITO, the current coatings can be used for ITO replacement in ionic reactive environments as well as smart windows, flexible displays, solar cells, and other comparable devices.

RESULTS AND DISCUSSION

Preparation and Structure. The selection of SWNTs poses practical importance on creating high-performance TCs

because their intrinsic properties critically depend on their manufacturers. The level of defect structure and chiral composition of original nanotubes strongly influence the TC performances. Hence information regarding the choice of SWNT source and subsequent method of their processing is quite relevant for this discussion. SWNTs made by high-pressure CO conversion (HiPCO) process have been widely tested by well-established experimental procedures. On the other hand it is reported that, SWNTs by electrical arc discharge (EA) production showed higher performance in TC applications.[20,33] Thus, we compared two different SWNTs in the experiments: HiPCO nanotubes from Carbon Nanotechnologies Incorporated (CNI, now Unidym) and EA SWNTs from Carbon Solution Co. (C-Sol, P-2). The property differences of two SWNTs originate from inherent structural variations during their synthesis including distribution of diameters, chiralities, lengths, graphitization, and electronic types. In addition, functional dopants and remnant impurities as high as 10% of SWNT contents during their purification process spread their dissimilarities. Among these, the average lengths of two types of SWNTs are remarkable. From our microscopy observations, C-Sol SWNTs were even several times longer than those from CNIs. Dispersion behavior with stabilizers and resulting optical properties were also quite different for SWNTs from CNI and C-Sol.

One advantage of LBL assemblies over conventional solution casting is conserving the dispersion quality of nanobuilding blocks from a solution to a solid state. Once we prepare exfoliated SWNT dispersions, multifunctional properties can be transferred and tailored to a macroscale film by LBL assemblies with precision.[15] Thus, the selection of stabilizers, either polyelectrolytes or surfactants, determines the effectiveness of SWNT's nanoscale structural organization and the ability to reach the desirable properties with respect to conductivity, transparency, and strength. Understanding the roles of stabilizers in SWNT TC applications is still fairly poor because stabilizers were simply considered to be impurities hampering free movement of charge carriers in percolation-type conduction routes. Thus, previous efforts have been focused on removing residual stabilizers in SWNT networks by rinsing,[6] heating,[6,32] and chemical treatment.[16,30] Certainly, this removal of stabilizers was believed to be appropriate stream in TC research until the multifunctional properties, including mechanical durability, flexibility, and even stretchability, are emerged as critical factors in wide ranges of the next generation of TC applications. Thus, we correlated the TC performances and the role of stabilizers during the molecular LBL assemblies, which can both improve and degrade TC performance and related figures of merit. The roles of the stabilizers include increasing SWNT's solvation in water by shielding hydrophobic side walls of SWNTs, preserving graphitization of nanotubes which affect electronic band structures, helping *in situ* doping effectiveness, and improving mechanical and environmental durability. In addition, these stabilizers also serve as molecular binders that make the surface smooth and significantly reduce micropores causing deteriorative light scattering in SWNT TC coatings. On the other hand, a very thick film of the stabilizer will render electrical transport impossible and hence all the other improvements irrelevant.

Optical Properties. Let us consider CNI dispersions first. Both poly(sodium 4-styrene sulfonate) (PSS) and sodium dodecyl sulfate (SDS) are effective stabilizers of SWNT dispersions (Figure 1A). UV−vis absorbance spectra of SWNT dispersions with these stabilizers showed van Hove singularity peaks indicative of a high degree of nanotube exfoliation. Comparing peaks' positions and shapes in the spectra, the SWNTs by PSS (CNI/PSS) showed sharper and more blue-shifted peaks than the ones dispersed by SDS (CNI/SDS). Similarly, it is perceived that high molecular weight PSS (1 M) produced slightly better exfoliation than lower molecular PSS (200 K) (Figure 1B).

The degree of exfoliation in a thin film coating and that in solution is expected to go in parallel because the dispersion qualities are conserved by LBL assembly. Indeed, substantial difference of the SWNT bundle sizes for two stabilizers was noticed in the LBL films (Figure 2A,B). SDS (CNI/SDS) produced 2−5 times larger SWNT bundles in diameter than PSS did. The diameters estimated from the SEM images were less than 10 nm and around 10−50 nm for PSS and SDS samples, respectively. Furthermore, the bundle sizes influence the light transmittance (T, $T/100 = 10^{-\alpha}$) patterns during LBL assemblies. The transmittances, measured at $\lambda = 550$ nm, of 10 bilayered LBL films were $T = 95 \pm 0.5\%$ for less bundled CNI/PSS *versus* $T = 83 \pm 0.5\%$ for more bundled CNI/SDS. Greater degree of bundling causes coupling of SWNT−SWNT electronic states, leading to stronger adsorption in the visible range[12,13,15] for dispersions and composites.

Now let us analyze UV−vis absorbance spectra of C-Sol SWNT dispersions, which showed both similarities and differences with those from CNI. C-Sol SWNT dispersions did not show van Hove singularities (Figure 1B), which may be indicative of thicker bundling as well as inherent structural differences. These bundling effects are confirmed in the SEM images (Figure 2C,D). Their bundles are around 10−20 and 10−60 nm for C-Sol/PSS and C-Sol/SDS, respectively. Exfoliation of longer C-Sol nanotubes is not efficient as the shorter CNI nanotubes most likely due to substantially stronger cooperative hydrophobic and π-system interactions. However, the trend of stabilizer effectiveness for C-Sol SWNTs is still the same as for CNI SWNTs. The light transmittances at $\lambda = 550$ nm of LBL coatings made after 10 deposition cycles with PSS and SDS were found

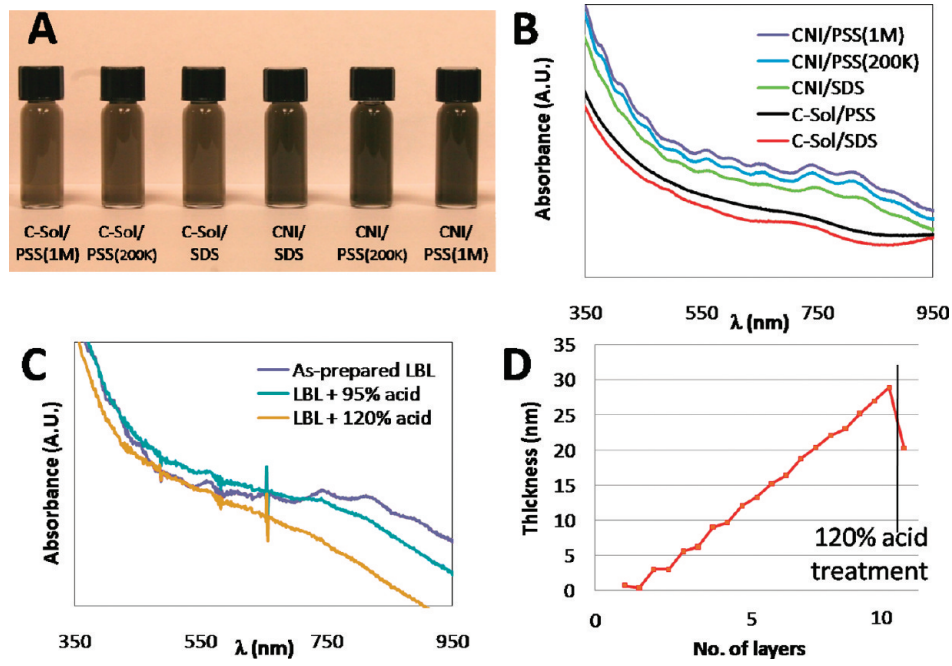

Figure 1. (A) Photographs of dispersions of C-Sol and CNI SWNTs with PSS (1 M, 200 K) and SDS stabilization used in the experiments. (B) UV−vis spectra of solutions in A. (C) UV−vis spectra of [PVA/CNI SWNTs + PSS (1 M)] LBL TC films before and after treatment by 95 and 120% H_2SO_4 (percentage of H_2SO_4 solution was calculated as excess SO_3^- concentration). (D) Ellipsometry thickness measurements of $[PVA/C\text{-}Sol\ SWNTs + PSS\ (1\ M)]_n$.

to be $T = 86 \pm 0.5\%$ and $T = 82 \pm 0.5\%$, respectively. Again, as the diameter of bundles visible in SEM increased, transparencies deteriorated fast.

Structural Characterization. Along with the optical properties, it is also informative to analyze the thickness of LBL films to understand both stabilizers and SWNTs better in LBL assemblies. The thickness of a layer deposited in one cycle depends on the size of molecules because each layer forms by a monomolecular stack. As such, the thickness of a SWNT LBL film is determined by a function of average diameter of SWNTs and roughness of surfaces where SWNTs are adsorbed. The average thickness of 1 bilayer of $[PVA/C\text{-}Sol + PSS\ (1\ M)]_n$ LBL was 3 nm: 2.2 nm for C-Sol/PSS (1 M) and 0.8 nm for PVA (Figure 1D). Analogously, the average thickness of LBL coating by $[PVA/CNI + PSS\ (1\ M)]_n$ was 2.24 nm: 1.77 nm for CNI/PSS (1 M) and 0.47 nm for PVA.[15] This correlates quite well with the generally observed SWNT's diameter range, which is 1.3−1.7 nm for EA produced SWNTs and 0.7−1.3 nm for HiPCO SWNTs.[34] The thickness of polymer binders including stabilizer, PSS wrapping, and PVA is projected then to be ~1−1.5 nm.

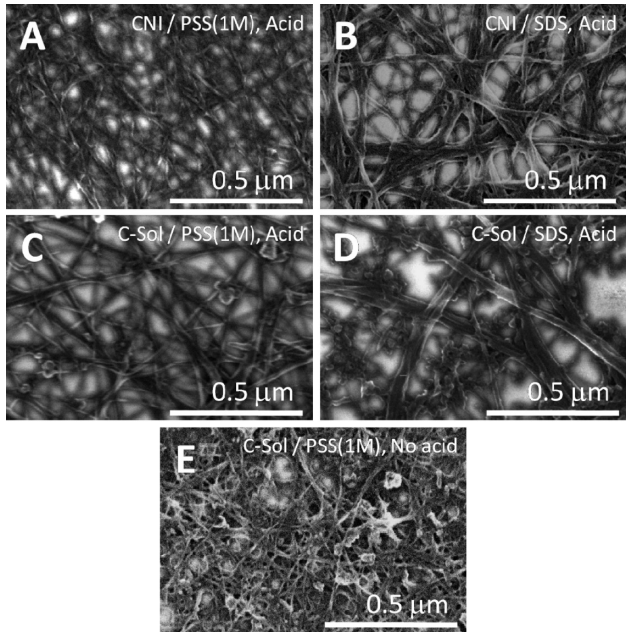

Figure 2. SEM images of (A) $[PVA/CNI\ SWNT + PSS\ (1\ M)]_{10}$ (T = 95%) LBL film after 120% H_2SO_4 super treatment, (B) $[PVA/CNI\ SWNT + SDS]_{10}$ (T = 83%) LBL film after 120% H_2SO_4 superacid treatment, (C) $[PVA/C\text{-}Sol\ SWNT + PSS\ (1\ M)]_{10}$ (T = 86%) LBL film after 120% H_2SO_4 superacid treatment, and (D) $[PVA/C\text{-}Sol\ SWNT + SDS]_{10}$ (T = 82%) LBL film after 120% H_2SO_4 superacid treatment, (E) $[PVA/C\text{-}Sol\ SWNT + PSS\ (1\ M)]_{10}$ LBL film before acid treatment.

Electrical Properties. Even a single layer of well-adsorbed SWNTs provides complete conduction percolative paths in LBL assemblies. Thus, the sheet resistance (R_s, Ω/sq) drops quickly as more SWNT layers are deposited. However, the as-formed LBL composite is not efficiently structured to utilize full conduction capacities of nanotubes because SWNTs are loosely bound in and between LBL layers. Thus, annealing structures are essential to enhance the electrical properties of a SWNT LBL film. Previously, we reported that tighter SWNT contacts formed by thermal annealing at 300 °C increased more than an order of magnitude of electrical conductivities of [CNI SWNT/PSS] LBL thin films. In TC applications, however, acid treatments such as 70% HNO_3[16,26] and 97% $SOCl_2$[30,35] were usually used to increase the electrical performances analogously.

TABLE 1. Summary of the Electrical Property Changes of CNI SWNT LBL Films by 120 and 95% H_2SO_4 Acid Treatments

	as-assembled		120% H_2SO_4 treatment		95% H_2SO_4 treatment	
samples	R_s (Ω/sq)	T (%)	R_s (Ω/sq)	T (%)	R_s (Ω/sq)	T (%)
$[PVA/CNI + PSS (1 M)]_{10}$	50500	93.1	1010	93.3	1620	92.8
$[PVA/CNI + SDS]_{10}$	2425	83.3	506.2	83.1	882.5	81.3

Here, we introduce a superacid (120% H_2SO_4) treatment annealing at room temperature, which alters the micro- and nanostructure of a LBL film by strong dehydration and modification of nanotube−polymer interactions. Chemical doping of SWNTs also takes place in acid media, which leads to higher effective charge carrier concentrations in SWNT networks.[36] The effect of superacid on the structure of a LBL film can be identified from SEM images (Figure 2C,E). One can see dramatic changes in coating structures: smoother SWNT side walls, larger voids, and removal of impurities, which is discussed in greater detail below.

To understand this superacid treatment effect in greater detail, CNI SWNT LBL films were analyzed first. The TC properties of as-prepared [PVA/CNI SWNTs + PSS (1 M)]$_{10}$ and [PVA/CNI SWNTs + SDS]$_{10}$ LBL films were 50.5 kΩ at T = 93.1% (TCFM = 0.00064 Ω^{-1}) and 2.43 kΩ at T = 83.3% (TCFM = 0.0052 Ω^{-1}). After superacid treatment, these values changed to 1.01 kΩ at T = 93.3% (TCFM = 0.033 Ω^{-1}) and 0.51 kΩ at T = 83.1% (TCFM = 0.024Ω^{-1}), respectively. If comparing with 95% H_2SO_4 treatment, these values were 1.62 kΩ at T = 92.8% (TCFM = 0.019 Ω^{-1}) and 0.88 kΩ at T = 81.3% (TCFM = 0.013 Ω^{-1}), respectively (Table 1). Evidently, the super concentration of H_2SO_4 acid brought in some degree of surplus effects on both optical and electrical properties.[16,26,30,35]

The acid concentration effects were rationalized based on the light absorbance spectra (Figure 1C). Both 120 and 95% H_2SO_4 caused absorbance drop at the S22 transitions in the range of 700−900 nm and eliminated the corresponding peaks in the region. These are typical for p-type ion doping transitions of SWNTs[36,37] caused by down-shifting of the Fermi level, E_F.[37] One can speculate based on the data that intercalated SO_3/SO_4^{2-} dopants facilitate occurrence of highly doped metallic behaving SWNTs more effectively than NO_3^- doping.[37,38] Recently, Nirmalraj *et al.* reported that these acid treatments could also significantly lower SWNT junction resistances, which are major leakages of conductivity in network forms.[39] The super acid, 120% H_2SO_4, furthermore, increased not only electrical conductivity but also optical transmittance (Figure 1C). Presumably, superacid removes some of polymeric components if not completely and therefore partially reconstructs the network to form tighter SWNT contacts. According to the ellipsometry measurements, the treatment reduces the thickness of original SWNT LBL film by about one-third (Figure 1D). One should note that single-stranded SWNTs with ohmic contacts have the potential ability of ballistic carrier transport like 1D quantum wires or electron waveguides,[10,40] although bundles of them or MWNTs show diffusive carrier characteristics.[8,41] XPS analysis of the SWNT LBL films before and after superacid treatment revealed that sulfur and oxygen content increased from 0.7 to 2.6% and 20.3 to 23.3%, respectively (Figure 3). It confirms that a substantial amount of guest SO_3/SO_4^{2-} dopants were intercalated in the film to affect SWNT's electronic state.

Then, we maximized TC performances of a SWNT LBL film by integrating this superacid treatment into the C-Sol SWNT LBL processes. The LBL films were treated every 5 bilayers by the superacid. At the same time, stabilizers such as PSS (1 M), PSS (200 K), and SDS were also compared (Figure 4A) As a result, TCFMs with PSS (1 M), PSS (200 K), and SDS were 0.104, 0.052, and, 0.023 Ω^{-1}, respectively. Interestingly, superacid doping was more effective for PSS with greater M_w. This observation substantiates the idea of partial removal of weakly bound polymeric material by superacid and, therefore, reduction of nanotube−nanotube gaps. For further optimization of superacid treated TC performance, we compared the weight ratio of SWNTs and PSS (1 M) by 1:1, 1:2, and 1:5 in SWNT dispersions (Figure 3B). Although this comparison is less significant, 1:2 in SWNT/PSS ratio showed the lowest resistivity trends. Thus, the optimally conditioned [PVA/C-Sol SWNT +

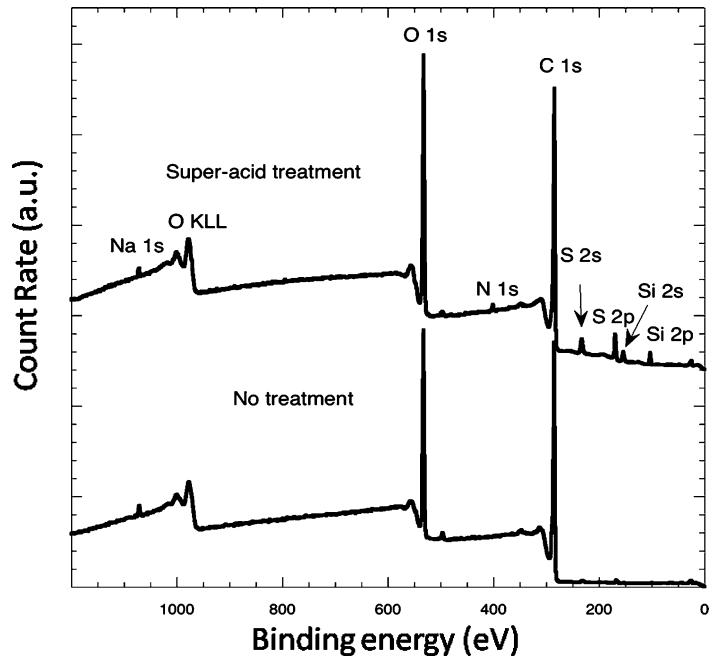

Figure 3. XPS results of [PVA/C-Sol SWNT + PSS (1 M)] LBL films before and after acid treatment.

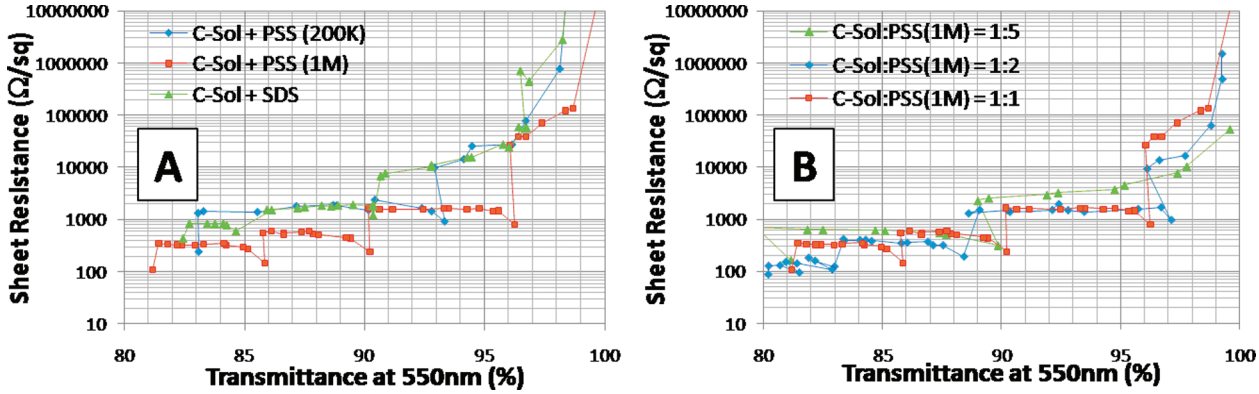

Figure 4. Comparisons of TC performances in (A) $[PVA/C\text{-}Sol\ SWNT + PSS\ (1\ M)]_n$, $[PVA/C\text{-}Sol\ SWNT + PSS\ (200\ K)]_n$, and $[PVA/C\text{-}Sol\ SWNT + SDS]_n$ LBL films and (B) SWNT:PSS weight ratios 1:5, 1:2, 1:1 of $[PVA/C\text{-}Sol\ SWNT + PSS\ (1\ M)]_n$ LBL films. All of the films were treated by superacid (120% H_2SO_4) every 5 bilayers. Please note the logarithmic scale of the ordinates in both graphs.

PSS (1 M)] LBL nanocomposite showed $R_s = 86\ \Omega$/sq with $T\ (\lambda = 550\ nm) = 80.2\%$ (TCFM $= 0.12\ \Omega^{-1}$), which is similar to the state-of-the-art SWNT TC coatings.[16,20,33,42] Hence, for all of the subsequent experiments aimed at versatile TC material performances, we used this particular family of coatings. For comparison, the TCFMs of recently reported representative SWNT TCs from Geng *et al.*,[16] Zhang *et al.*,[20] De *et al.*,[33] and Saran *et al.*[42] were 0.16, 0.103, 0.1, and 0.13 Ω^{-1}, respectively. However, in the framework of flexible polymeric composites, this study showed the best performing system based on our limited knowledge.[33]

It might also be useful to compare the performance of SWNT LBL coatings with benchmarks used in electronics industry. To use TCs in touch screen displays, one needs at least $R_s = 500\ \Omega$/sq with $T\ (\lambda = 550\ nm) = 85\%$.[16] Many other applications require $R_s = 100\ \Omega$/sq with $T\ (\lambda = 550\ nm) = 90\%$.[33] In this respect, the produced coatings are very suitable for practical applications in many fields. LBL process can be easily scaled-up without potential cost/quality deterioration. The current performance parameters are, in principle, sufficient for many TC applications. However, much work still needs to be done to establish compatibility with electronic and chemical properties of other materials.

Protective Capping Layers. TC performance obtained after chemical treatment typically deteriorates with time due to the volatility of dopants (dedoping).[43] In a 24 h period, the resistivity of $[PVA/C\text{-}Sol\ SWNT + PSS\ (1\ M)]_{10}$ LBL film with superacid treatment increased more than 40% from its original value. In order to reduce this dedoping effect, a nanothin transparent impermeable capping layer, $[PVA/Clay]_3$ LBL assembly, was formed to protect the TC performance. When we added this clay capping layer on the SWNT LBL TCs, the resistivity slightly increased. However, after restoring the doping with the same superacid treatment, the resistivity drops even *below the original value* (Figure 5A). Resistance continued to decrease as we added more clay capping layers (Figure 5A). This was quite unexpected, and the reason for this improvement of electrical characteristics of TC by addition of clay (which is an insulator) is not well-understood at the moment. It is possible that clay serves as an *in situ* dopant "storing" acid groups in nonvolatile form and the clay layers filled with acid dopants behave as a solid electrolyte with ionic conduction. The protective functionality of this impermeable clay layers was demonstrated in the same 24 h period. The

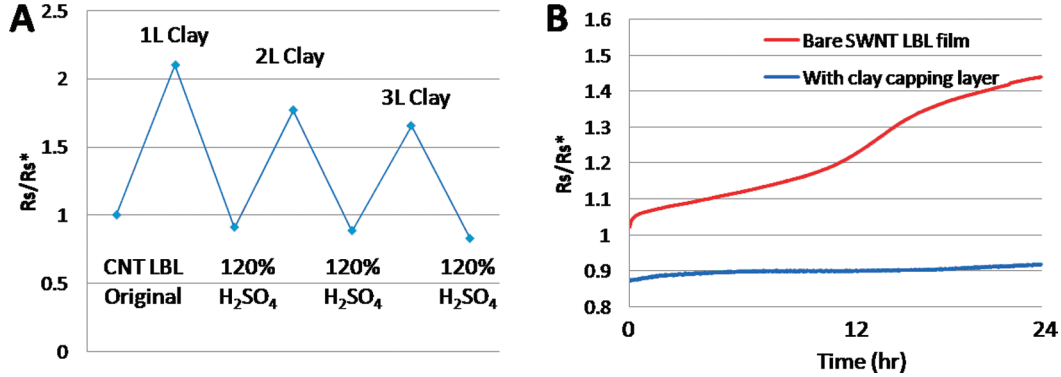

Figure 5. (A) Electrical sheet resistance (R_s) measurements during [PVA/Clay] LBL capping layer and 120% H_2SO_4 processing. (B) Electrical resistance change of SWNT LBL films, $[PVA/C\text{-}Sol\ SWNT + PSS\ (1\ M)]_{10}$ (120% H_2SO_4 treatment every 5 bilayers) with and without clay capping layers, $[PVA/clay/120\%\ H_2SO_4]_3$ in 24 h. R_s* indicates the electrical resistance of bare SWNT TC coating right after 120% H_2SO_4 treatment.

increase of resistance due to dedoping was significantly suppressed (Figure 5B). Although blue-black semitransparent PEDOT:PSS capping layers were tried previously,[43] the clay LBL layers are more appropriate choices in TC applications because of their nearly perfect transparency and exceptional strength.[44] The optical transmittance of a CNT LBL composite remains the same even after multiple additions of clay LBL layers.

Bending Properties. For most up and coming practical applications, TC bending performance is particularly important. Some other parameters, such as tensile strength and toughness, characterizing stretchability and wear resistance can also be considered as well but are either more application specific or less challenging to improve than mechanical properties of TCs in bending. In a simple case of uniaxial bending, the outer and the inner layers are in tension and in compression, respectively. The strain of a component layer in a film can be estimated as $\varepsilon = y/R$, where ε = strain, y = the distance from the neutral axis layer (aka the zero deformation axis), and R = radius of the bending curvature.[45]

Considerable efforts have been invested in the past into the design of multilayer TC films where the most critical brittle (oxide) material is located along the neutral axis of bending. However, it is impractical for every brittle material to locate in the center of the film. More importantly, the flexural deformations in modern devices are often multiaxial resulting in complex strain distribution patterns, which makes this approach often much more difficult to implement.

Overall, the brittleness of ITOs and similar semiconducting components critically limits the flexibility of the entire device and is the primary cause of the device failure. The measures of ITO's brittleness are usually represented by critical strain (ε_c), R, and number of bending cycles (n). Their values vary by the substrate, buffer layers, and coating conditions of testing ITOs. In terms of ε_c, there are two techniques to determine it. One is measuring the onset of cracks on the surface. The other is finding the point of inflection of the strain−resistance curve. The critical strain, ε_c, by either ways represents a maximum strain before electrical failure, which causes a device malfunction. Chen *et al.* reported that the ε_c of 100 nm thick ITO coating on a PET substrate was 1.1% for tension and 1.7% for compression.[45] The strains of ITOs are strongly dependent on the film thickness. Leterrier *et al.* found that the crack onset strain varied from 0.83% (200 nm thick) to 1.69% (50 nm thick).[46] This strain corresponds to around 1 cm as minimum allowable radius of bending curvature at their best design when the substrate was 100−200 μm.[47,48] For estimating bending cycles, there is no simple indicator, but it is demonstrated by a plot of resistance change and cycle numbers at their minimum radius of bending curvature. Although conventional bare ITO is very poor at this repeated bending, some treatments, such as Ag backing layers[49] or pulse magnetron sputtering[50] could improve their repeated bending cycles up to 10^5 times. Overall, the current state of ITOs is severely limited for their use in flexible electronics due to low ε_c, which causes high minimum allowable radius of bending curvature.

We tested mechanical properties of SWNT LBL film following the terms of ITO coatings. The ε_c of [PVA/C-Sol SWNT + PSS (1 M)]$_{10}$ LBL film coated on a 230 μm polystyrene (PS) substrate was 99 and 120% before and after superacid treatment, respectively (Figure 6A). This value indicates *ca.* 100 times improvements in their bending performances compared to ITOs. The resistance changes in low strain ranges up to 5 mm bending radius of both stretching and compression are shown in Figure 6B−D. The causes of these high bending properties are flexible polymeric binders as well as slight in-plane buckling effect of SWNTs when they are adsorbed in a soft PS substrate[51] (Supporting Information Figure 1). Importantly, the described LBL TC films can be easily deposited on a large-scale letter paper size plastic substrate in our laboratory (Figure 7B).

New Figure of Merit for Flexible TCs. We believe that the area of flexible electronics and other applications of TCs will be better served by introducing mechanical properties into consideration. In our opinion, the mechanical properties must be given equal weight with optical transparency and conductivity when considering the suitability of a particular material for TC applications, which had not be done before. Therefore, we would like to introduce a new figure of merit for flexible TCs, which reflects the new technological realities of mechanical properties for the practical prospects of materials. Considering the specific needs of the flexible electronics, touch screen displays, wearable sensors, and similar applications when the material is bent, worn, stretched, and compressed extensively, one probably needs to use a parameter which reflects the best flexible durability of the material, which is critical strain, ε_c. Therefore, we propose to evaluate flexible TC materials using the new figure of merit according to the following equation

$$\Pi_{TC} = \sigma\varepsilon_c/\alpha \quad (\Omega^{-1}) \tag{1}$$

which gives the cumulative estimate of the properties relevant for flexible TCs better than TCFM used before. Note that other mechanical parameters can also be included in this formula, for instance, tensile strength, toughness, or Young's modulus. This certainly can be considered depending on how critical this parameter is. Similarly, the more extensive description of optical or electrical properties can be used, as well. As such, transparency at several wavelengths can be incorporated. Our suggestion is to use the simplest variant of eq 1 at the moment.

With respect to the new figure of merit, the SWNT LBL films give $\Pi_{TC} = 0.15\ \Omega^{-1}$, whereas Π_{TC} of the conventional ITO coatings is lower than $0.07\ \Omega^{-1}$. Note that

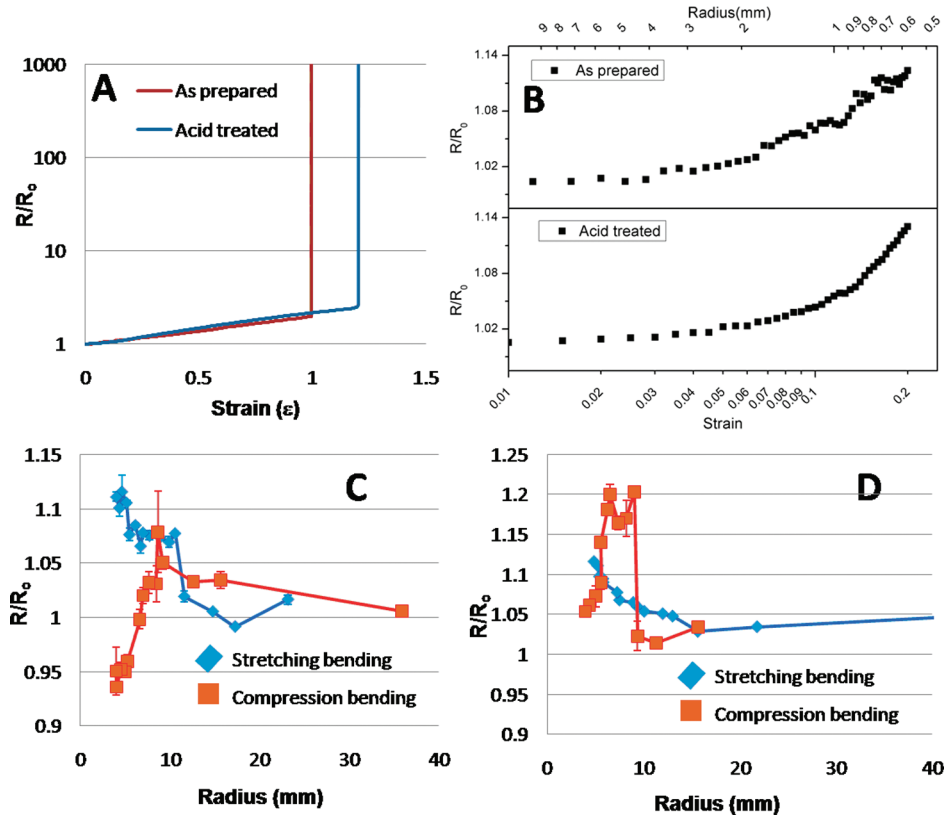

Figure 6. (A−D) Electrical resistance changes of [PVA/C-Sol SWNT + PSS (1 M)]$_{10}$ LBL films coated on a flexible 230 μm thick PS substrate. (A) Coated films with and without superacid treatment are stretched until electrical network paths are broken. (B) Correlations between bending radius and stretching strain are shown in the same plots. These direct stretching results provide universal trends of TC's bending performances. (C,D) Electrical resistance changes by actual stretching and compression bending experiments of the coated films (C) without and (D) with superacid treatment were shown. These actual bending results are critically dependent on the thickness of a substrate as well as adherence of SWNT coating on a substrate. Here, R_o indicates the resistance at no strain.

Π_{TC} of bucky-paper-like SWNT TC networks may be much lower than those because the strain at breaking is less than 6%.[26] The comparison between ITO and SWNT coatings is indeed quite revealing. Despite the indication of overall better performance, the cumulative figure is not as high as one might expect based on mechanical performance, which may be considered as the clue for further improvement both optical and electrical characteristics.

CONCLUSION

The ability to finely tune the nanoscale organization in the composites allowed SWNT LBL films to demonstrate competitive TC performance in terms of electrical/optical properties and exceptional performance in terms of mechanical properties. We demonstrated that the combination techniques of suitable polymeric stabilizers, exfoliated conductive SWNTs, assemblies controlled at the nanoscale, and efficient post treatments can not only produce viable TC coatings but also actually match or improve electrical parameters compared to the state-of-the-art SWNT TC systems. Molecularly thin polymeric binders between SWNT layers significantly improve mechanical stability, and clay capping LBL layers can protect TC performance without sacrificing optical transparency.

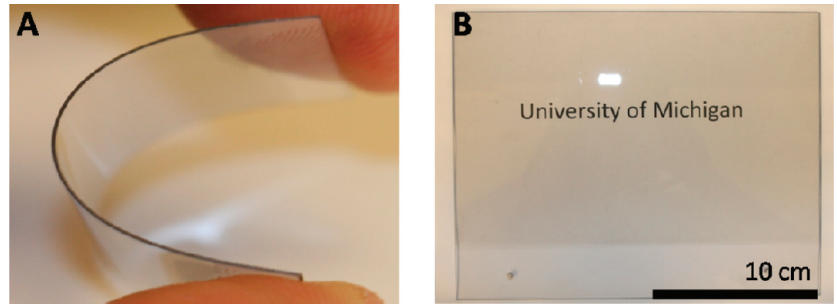

Figure 7. Photo images of (A) bending of the SWNT LBL coating on the PS substrate and (B) large-scale coating of a SWNT LBL TC film.

Consistent with the new technological realities of TC applications, a new figure of merit to evaluate the performance of different materials for flexible transparent conductive coatings was introduced. The new expression includes critical bending strain of the material as one of the three key parameters and basically states that mechanical properties are equally important for TC performance as optical and electrical properties. The new figure of merit Π_{TC} was calculated for [PVA/C-Sol SWNT + PSS (1 M)]$_n$ coatings and compared to those for other traditional TCs. The expression for the new figure of merit is quite universal and can be extended to incorporate other relevant properties when necessary.

METHODS

Materials. Poly(vinyl alcohol) (PVA, MW 9000), poly(sodium 4-styrene sulfonate), (PSS, MW 200 000, PSS (200 K) and 1 000 000, PSS (1 M)), and sodium dodecyl sulfate (SDS) were purchased from Sigma-Aldrich Co. SWNTs were purchased from Carbon Nanotechnologies Incorporated (purified HiPco SWNTs; now the company merged with Unidym) (CNI SWNTs) and Carbon Solution Co. (P-2, SWNTs) (C-Sol SWNTs); 95% sulfuric acid (95% H_2SO_4), 120% super sulfuric acid (H_2SO_4, fuming, 20% free SO_3 basis), glutaraldehyde, and HF were purchased from Sigma-Aldrich Co.

LBL Assembly. SWNTs were dispersed in water with negatively charged stabilizers such as PSS and SDS. PVA solutions (0.2%) were prepared. By charge transfer interaction between SWNTs and PVA, or by hydrogen bonding between possible COOH groups in SWNTs and OH in PVA, they formed LBL assemblies on a charged substrate (glass, Si, or polystyrene). Each LBL layering process consists of dipping in the PVA and the SWNT solution, rinsing in deionized (DI) water, and drying. To denote LBL assemblies, [PVA/SWNT (CNI or C-Sol) + stabilizer (PSS or SDS)]$_n$ was used in which n represents the number of repeated dipping processes in PVA and SWNT solutions.

As post treatments, the films were dipped in acids (95 and 120% H_2SO_4) for 2 min. The 95% sulfuric acid treated sample was rinsed in DI water and dried. The 120% sulfuric acid treated sample was rinsed shortly in 95% sulfuric acid and then rinsed in DI water and dried. Users should give special attention because 120% sulfuric acid reacts with water explosively. For clay capping layers, the existing SWNT LBL films were processed by [PVA/Clay] LBL dipping steps and 120% H_2SO_4 treatments. A 0.5% clay solution was used here. The detailed procedures for clay LBL assemblies are described in a previous publication.[44]

Free-standing LBL films were prepared by repeating 200 times of the same dipping procedures. The LBL films were detached by dipping in 1% HF solutions. Before film detachment, the film was cross-linked in 5% glutaraldehyde to prevent polymer swelling.

Instrumental Analysis. Scanning electron microscopy (SEM) images were taken using a Philips XL30 field emission gun scanning electron microscope and an FEI Nova Nanolab dual-beam FIB and scanning electron microscope. Atomic force microscopy (AFM) imaging was performed using a Nanoscope III (Digital Instruments/Veeco Metrology Group). UV−vis absorption measurements were taken using an Agilent 8453E UV−visible spectroscope. An Agilent 34401A multimeter was used for electrical measurements. Mechanical tests were done by Q systems model 100 (Test Resources). Thermogravimetric analysis (TGA) was performed using a PerkinElmer Pyris 1 TGA. Ellipsometric measurements were done with a M-44 IR spectroscopic ellipsometer (J.A. Woollam Co., Inc.). X-ray photoelectron spectroscopy (XPS) was carried out using a Kratos Axis Ultra. A monochromated Al Kα X-ray source was used to irradiate the sample using a power of 140 W (14 kV, 10 mA). A chamber pressure of better than 1×10^{-9} was maintained throughout the experiment. Survey scans were performed using a pass energy of 160 eV, a step size of 1 eV, and a dwell time of 200 ms. Detailed scans were acquired with a pass energy of 20 eV, a step size of 0.1 eV, and a dwell time of 200 ms. A flood gun was used for charge compensation.

Supporting Information Available: Additional figures. This material is available free of charge *via* the Internet at http://pubs.acs.org.

REFERENCES AND NOTES

1. Baedeker, K. Electrical Conductivity and Thermoelectric Power of Some Heavy Metal Compounds. *Ann. Phys.* **1907**, *22*, 749–766.
2. Gordon, R. G. Criteria for Choosing Transparent Conductors. *MRS Bull.* **2000**, *25*, 52–57.
3. Cao, Q.; Rogers, J. A. Ultrathin Films of Single-Walled Carbon Nanotubes for Electronics and Sensors: A Review of Fundamental and Applied Aspects. *Adv. Mater.* **2009**, *21*, 29–53.
4. Ko, H. C.; Stoykovich, M. P.; Song, J. Z.; Malyarchuk, V.; Choi, W. M.; Yu, C. J.; Geddes, J. B.; Xiao, J. L.; Wang, S. D.; Huang, Y. G.; Rogers, J. A. A Hemispherical Electronic Eye Camera Based on Compressible Silicon Optoelectronics. *Nature* **2008**, *454*, 748–753.
5. Chipman, A. A Commodity No More. *Nature* **2007**, *449*, 131.
6. Wu, Z.; Chen, Z.; Du, X.; Logan, J. M.; Sippel, J.; Nikolou, M.; Kamaras, K.; Reynolds, J. R.; Tanner, D. B.; Hebard, A. F.; Rinzler, A. G. Transparent, Conductive Carbon Nanotube Films. *Science* **2004**, *305*, 1273–1277.
7. Gruner, G. Carbon Nanotube Films for Transparent and Plastic Electronics. *J. Mater. Chem.* **2006**, *16*, 3533–3539.
8. Fischer, J. E.; Dai, H.; Thess, A.; Lee, R.; Hanjani, N. M.; Dehaas, D. L.; Smalley, R. E. Metallic Resistivity in Crystalline Ropes of Single-Wall Carbon Nanotubes. *Phys. Rev. B: Condens. Matter* **1997**, *55*, 4921–4924.
9. Panhuis, M. I. H. Carbon Nanotubes: Enhancing the Polymer Building Blocks for Intelligent Materials. *J. Mater. Chem.* **2006**, *16*, 3598–3605.
10. Mann, D.; Javey, A.; Kong, J.; Wang, Q.; Dai, H. J. Ballistic Transport in Metallic Nanotubes with Reliable Pd Ohmic Contacts. *Nano Lett.* **2003**, *3*, 1541–1544.
11. Lewis, B. G.; Paine, D. C. Applications and Processing of Transparent Conducting Oxides. *MRS Bull.* **2000**, *25*, 22–27.
12. Hu, L.; Hecht, D. S.; Gruener, G. Percolation in Transparent and Conducting Carbon Nanotube Networks. *Nano Lett.* **2004**, *4*, 2513–2517.
13. Unalan, H. E.; Fanchini, G.; Kanwal, A.; Du Pasquier, A.; Chhowalla, M. Design Criteria for Transparent Single-Wall Carbon Nanotube Thin-Film Transistors. *Nano Lett.* **2006**, *6*, 677–682.
14. Vigolo, B.; Coulon, C.; Maugey, M.; Zakri, C.; Poulin, P. An Experimental Approach to the Percolation of Sticky Nanotubes. *Science* **2005**, *309*, 920–923.
15. Shim, B. S.; Tang, Z.; Morabito, M. P.; Agarwal, A.; Hong, H.; Kotov, N. A. Integration of Conductivity, Transparency, and Mechanical Strength into Highly Homogeneous Layer-by-Layer Composites of Single-Walled Carbon Nanotubes for Optoelectronics. *Chem. Mater.* **2007**, *19*, 5467–5474.
16. Geng, H. Z.; Kim, K. K.; So, K. P.; Lee, Y. S.; Chang, Y.; Lee, Y. H. Effect of Acid Treatment on Carbon Nanotube-Based Flexible Transparent Conducting Films. *J. Am. Chem. Soc.* **2007**, *129*, 7758–7759.
17. Barnes, T. M.; de Lagemaat, J. V.; Levi, D.; Rumbles, G.; Coutts, T. J.; Weeks, C. L.; Britz, D. A.; Levitsky, I.; Peltola, J.; Glatkowski, P. Optical Characterization of Highly Conductive Single-Wall Carbon-Nanotube Transparent Electrodes. *Phys. Rev. B* **2007**, *75*, 235410.
18. Meitl, M. A.; Zhou, Y. X.; Gaur, A.; Jeon, S.; Usrey, M. L.;

Strano, M. S.; Rogers, J. A. Solution Casting and Transfer Printing Single-Walled Carbon Nanotube Films. *Nano Lett.* **2004**, *4*, 1643–1647.
19. Lima, M. D.; de Andrade, M. J.; Bergmann, C. P.; Roth, S. Thin, Conductive, Carbon Nanotube Networks over Transparent Substrates by Electrophoretic Deposition. *J. Mater. Chem.* **2008**, *18*, 776–779.
20. Zhang, D.; Ryu, K.; Liu, X.; Polikarpov, E.; Ly, J.; Tompson, M. E.; Zhou, C. Transparent, Conductive, and Flexible Carbon Nanotube Films and Their Application in Organic Light-Emitting Diodes. *Nano Lett.* **2006**, *6*, 1880–1886.
21. Kang, S. J.; Kocabas, C.; Ozel, T.; Shim, M.; Pimparkar, N.; Alam, M. A.; Rotkin, S. V.; Rogers, J. A. High-Performance Electronics Using Dense, Perfectly Aligned Arrays of Single-Walled Carbon Nanotubes. *Nat. Nanotechnol.* **2007**, *2*, 230–236.
22. Ma, W. J.; Song, L.; Yang, R.; Zhang, T. H.; Zhao, Y. C.; Sun, L. F.; Ren, Y.; Liu, D. F.; Liu, L. F.; Shen, J.; Zhang, Z. X.; Xiang, Y. J.; Zhou, W. Y.; Xie, S. S. Directly Synthesized Strong, Highly Conducting, Transparent Single-Walled Carbon Nanotube Films. *Nano Lett.* **2007**, *7*, 2307–2311.
23. Zhang, M.; Fang, S.; Zakhidov, A. A.; Lee, S. B.; Aliev, A. E.; Williams, C. D.; Atkinson, K. R.; Baughman, R. H. Strong, Transparent, Multifunctional, Carbon Nanotube Sheets. *Science* **2005**, *309*, 1215–1219.
24. Baughman, R. H.; Zakhidov, A. A.; de Heer, W. A. Carbon Nanotubes—The Route toward Applications. *Science* **2002**, *297*, 787–792.
25. Calvert, P. Nanotube Composites: A Recipe for Strength. *Nature* **1999**, *399*, 210–211.
26. Zhang, X.; Sreekumar, T. V.; Liu, T.; Kumar, S. Properties and Structure of Nitric Acid Oxidized Single Wall Carbon Nanotube Films. *J. Phys. Chem. B* **2004**, *108*, 16435–16440.
27. Sreekumar, T. V.; Liu, T.; Kumar, S.; Ericson, L. M.; Hauge, R. H.; Smalley, R. E. Single-Wall Carbon Nanotube Films. *Chem. Mater.* **2003**, *15*, 175–178.
28. Mamedov, A. A.; Belov, A.; Giersig, M.; Mamedova, N. N.; Kotov, N. A. Nanorainbows: Graded Semiconductor Films from Quantum Dots. *J. Am. Chem. Soc.* **2001**, *123*, 7738–7739.
29. Ostrander, J. W.; Mamedov, A. A.; Kotov, N. A. Two Modes of Linear Layer-by-Layer Growth of Nanoparticle-Polylectrolyte Multilayers and Different Interactions in the Layer-by-Layer Deposition. *J. Am. Chem. Soc.* **2001**, *123*, 1101–1110.
30. Parekh, B. B.; Fanchini, G.; Eda, G.; Chhowalla, M. Improved Conductivity of Transparent Single-Wall Carbon Nanotube Thin Films *via* Stable Postdeposition Functionalization. *Appl. Phys. Lett.* **2007**, *90*, 121913.
31. Geng, H. Z.; Kim, K. K.; Song, C.; Xuyen, N. T.; Kim, S. M.; Park, K. A.; Lee, D. S.; An, K. H.; Lee, Y. S.; Chang, Y.; Lee, Y. J.; Choi, J. Y.; Benayad, A.; Lee, Y. H. Doping and De-Doping of Carbon Nanotube Transparent Conducting Films by Dispersant and Chemical Treatment. *J. Mater. Chem.* **2008**, *18*, 1261–1266.
32. Yim, J. H.; Kim, Y. S.; Koh, K. H.; Lee, S. Fabrication of Transparent Single Wall Carbon Nanotube Films with Low Sheet Resistance. *J. Vac. Sci. Technol., B* **2008**, *26*, 851–855.
33. De, S.; Lyons, P. E.; Sorel, S.; Doherty, E. M.; King, P. J.; Blau, W. J.; Nirmalraj, P. N.; Boland, J. J.; Scardaci, V.; Joimel, J.; Coleman, J. N. Transparent, Flexible, and Highly Conductive Thin Films Based on Polymer−Nanotube Composites. *ACS Nano* **2009**, *3*, 714–720.
34. Green, A. A.; Hersam, M. C. Colored Semitransparent Conductive Coatings Consisting of Monodisperse Metallic Single-Walled Carbon Nanotubes. *Nano Lett.* **2008**, *8*, 1417–1422.
35. Dettlaff-Weglikowska, U.; Skakalova, V.; Graupner, R.; Jhang, S. H.; Kim, B. H.; Lee, H. J.; Ley, L.; Park, Y. W.; Berber, S.; Tomanek, D.; Roth, S. Effect of Socl2 Treatment on Electrical and Mechanical Properties of Single-Wall Carbon Nanotube Networks. *J. Am. Chem. Soc.* **2005**, *127*, 5125–5131.
36. Fischer, J. E. Chemical Doping of Single-Wall Carbon Nanotubes. *Acc. Chem. Res.* **2002**, *35*, 1079–1086.
37. Zhou, W.; Vavro, J.; Nemes, N. M.; Fischer, J. E.; Borondics, F.; Kamaras, K.; Tanner, D. B. Charge Transfer and Fermi Level Shift in p-Doped Single-Walled Carbon Nanotubes. *Phys. Rev. B* **2005**, *71*, 205423.
38. Graupner, R.; Abraham, J.; Vencelova, A.; Seyller, T.; Hennrich, F.; Kappes, M. M.; Hirsch, A.; Ley, L. Doping of Single-Walled Carbon Nanotube Bundles by Bronsted Acids. *Phys. Chem. Chem. Phys.* **2003**, *5*, 5472–5476.
39. Nirmalraj, P. N.; Lyons, P. E.; De, S.; Coleman, J. N.; Boland, J. J. Electrical Connectivity in Single-Walled Carbon Nanotube Networks. *Nano Lett.* **2009**, *9*, 3890–3895.
40. Javey, A.; Guo, J.; Wang, Q.; Lundstrom, M.; Dai, H. J. Ballistic Carbon Nanotube Field-Effect Transistors. *Nature* **2003**, *424*, 654–657.
41. Bachtold, A.; Fuhrer, M. S.; Plyasunov, S.; Forero, M.; Anderson, E. H.; Zettl, A.; McEuen, P. L. Scanned Probe Microscopy of Electronic Transport in Carbon Nanotubes. *Phys. Rev. Lett.* **2000**, *84*, 6082–6085.
42. Saran, N.; Parikh, K.; Suh, D. S.; Munoz, E.; Kolla, H.; Manohar, S. K. Fabrication and Characterization of Thin Films of Single-Walled Carbon Nanotube Bundles on Flexible Plastic Substrates. *J. Am. Chem. Soc.* **2004**, *126*, 4462–4463.
43. Jackson, R.; Domercq, B.; Jain, R.; Kippelen, B.; Graham, S. Stability of Doped Transparent Carbon Nanotube Electrodes. *Adv. Funct. Mater.* **2008**, *18*, 2548–2554.
44. Podsiadlo, P.; Kaushik, A. K.; Arruda, E. M.; Waas, A. M.; Shim, B. S.; Xu, J. D.; Nandivada, H.; Pumplin, B. G.; Lahann, J.; Ramamoorthy, A.; Kotov, N. A. Ultrastrong and Stiff Layered Polymer Nanocomposites. *Science* **2007**, *318*, 80–83.
45. Chen, Z.; Cotterell, B.; Wang, W.; Guenther, E.; Chua, S. J. A Mechanical Assessment of Flexible Optoelectronic Devices. *Thin Solid Films* **2001**, *394*, 202–206.
46. Leterrier, Y.; Medico, L.; Demarco, F.; Manson, J. A. E.; Betz, U.; Escola, M. F.; Olsson, M. K.; Atamny, F. Mechanical Integrity of Transparent Conductive Oxide Films for Flexible Polymer-Based Displays. *Thin Solid Films* **2004**, *460*, 156–166.
47. Park, S. K.; Han, J. I.; Moon, D. G.; Kim, W. K. Mechanical Stability of Externally Deformed Indium-Tin-Oxide Films on Polymer Substrates. *Jpn. J. Appl. Phys.* **2003**, *42*, 623–629.
48. Yu, Z. N.; Li, Y. Q.; Xia, F.; Zhao, Z. W.; Xue, W. Properties of Indium Tin Oxide Films Deposited on Unheated Polymer Substrates by Ion Beam Assisted Deposition. *Thin Solid Films* **2009**, *517*, 5395–5398.
49. Lewis, J.; Grego, S.; Chalamala, B.; Vick, E.; Temple, D. Highly Flexible Transparent Electrodes for Organic Light-Emitting Diode-Based Displays. *Appl. Phys. Lett.* **2004**, *85*, 3450–3452.
50. Lin, Y. C.; Shi, W. Q.; Chen, Z. Z. Effect of Deflection on the Mechanical and Optoelectronic Properties of Indium Tin Oxide Films Deposited on Polyethylene Terephthalate Substrates by Pulse Magnetron Sputtering. *Thin Solid Films* **2009**, *517*, 1701–1705.
51. Hur, S. H.; Park, O. O.; Rogers, J. A. Extreme Bendability of Single-Walled Carbon Nanotube Networks Transferred from High-Temperature Growth Substrates to Plastic and Their Use in Thin-Film Transistors. *Appl. Phys. Lett.* **2005**, *86*, 243502.